

Removal of various anionic dyes using sodium alginate/poly(*N*-vinyl-2-pyrrolidone) blend hydrogel beads

Murat İnal¹ · Nuran Erduran²

Received: 1 October 2013 / Revised: 15 February 2015 / Accepted: 23 March 2015 /
Published online: 31 March 2015
© Springer-Verlag Berlin Heidelberg 2015

Abstract In this study, novel blend hydrogel beads were prepared for the use in removal of anionic textile dyes due to their hazardous impact to nature. Sodium alginate and sodium alginate/poly(*N*-vinyl-2-pyrrolidone) beads were prepared by gelation method into calcium chloride solution. Prepared blend beads were characterized by TGA and FTIR analysis, and they were successfully used in adsorption of the reactive red-120 (RR), cibacron brilliant red 3B-A (CBR) and remazol brilliant blue R (RBB) in batch system. The effects of various parameters such as pH, initial dye concentration, contact time and temperature onto adsorption were investigated. The maximum adsorption capacities were found 116.8, 73.3 and 55.3 mg g⁻¹ for RR, CBR and RBB, respectively. The adsorption of dyes was well described by pseudo-second-order kinetics and Langmuir isotherm. Thermodynamic parameters indicated that the adsorption is spontaneous and exothermic. These results have shown that blend hydrogel beads can be effectively used as adsorbent in the removal of dyes from harmful wastewaters.

Keywords Hydrogel beads · Adsorption · Anionic dye · Sodium alginate · Poly(*N*-vinyl-2-pyrrolidone)

✉ Murat İnal
inalmrt@yahoo.com

¹ Department of Bioengineering, Faculty of Engineering, Kırıkkale University, 71450 Yahşihan, Kırıkkale, Turkey

² Department of Chemistry, Faculty of Science and Art, Kırıkkale University, 71450 Yahşihan, Kırıkkale, Turkey

Introduction

Nowadays, environmental pollutions have increased because of growth of human population and rapid development of industry. Organic based chemicals and effluents used in many industries are some of the most important factors of environmental pollution. Synthetic dyes and dyestuffs, which are a group of organic based chemicals, are generally used in miscellaneous areas such as textile, paper, printing, plastic, cosmetic, food and carpet [1, 2]. Approximately 20–40 % of dyes used in these industries are disposed in the nature with the wastewaters [3]. Many of dyes used in the textile industry and their degradation products (such as aromatic amines) may be toxic, carcinogenic, teratogenic and mutagenic for humans and aquatic organisms and in addition these can lead allergic reactions, skin irritation etc. temporary diseases in human body [4–6]. Also, waste dyes cause to an aesthetically disagreeable image on the water surface and decrease in photosynthesis and/or dissolved oxygen concentration depending on reduction of sunlight transition into the water [5, 7].

Dyes are composed from various groups such as acid, reactive, basic, cationic and nonionic-disperse dyes [8]. The reactive dyes are commonly used dyes in textile industry due to properties such as directly reacting with the cellulose fibers, bright color, and high water solubility, resistance against microbial attack, light stability and easy application [9]. They contain most functional groups such as azo, anthraquinone, chlorotriazine, vinyl sulfone, and vinyl amide [10]. They have high stability to chemical, photochemical, and biological degradation and thus, these dyes may still remain as waste in the natural environment [3]. Hence, removal of dyes is important for ecological balance and environmental problems. The physical, chemical, and biological processes have been used to removal of dyes in the wastewaters [11]. These treatment processes include chemical coagulation/flocculation, ozonation, chemical oxidation, photo oxidation, enzymatic decomposition, ion exchange, irradiation, membrane separation, electrochemical destruction, and adsorption [9, 12, 13]. Adsorption is one of the most effective techniques between these applications. This method has been used due to properties such as simplicity, high efficiency, cost effectively, recovery, and reusability [14]. Many adsorbents have been investigated, including activated carbon, inorganic or organic materials, biological materials, and polymers.

A natural polysaccharide, sodium alginate (NaAlg) derived from brown seaweeds, is composed of β -D-mannuronic acid and α -L-guluronic acid [15]. NaAlg has many important properties such as biocompatible, biodegradable, non-toxic, chelating able, gelable polysaccharide and suitable for chemical modification [16]. NaAlg can be formed as hydrogel beads and microspheres by cross-linking the guluronic acid units with di- or polyvalent cations. The use of the natural, biocompatible, non-toxic polymer hydrogels as adsorbent has been gradually increased. However, usability of many natural polymers are limited to use as an adsorbent due to some this disadvantages especially poor mechanical strength and microbial degradation. For enhancing usability of natural polymers can be usually blended by synthetic polymer(s) for semi interpenetrating polymer network

hydrogel. While semi interpenetrating network hydrogel beads are prepared with natural and synthetic polymers, convenient groups of natural polymer are cross linked. At the same time, synthetic polymer chains remains between crosslink networks of natural polymer. Because of is active in functional groups of synthetic polymers in polymeric network, the obtained hydrogel beads effectively may be used as an adsorbent [17–21].

Poly(*N*-vinyl-2-pyrrolidone) (PVP) is a non-toxic, biodegradable, biocompatible via hydrophilic polymer that shows water solubility with respect to polar organic solvents. Due to these advantages, PVP are favorable as blend hydrogels component. There are several studies related to the adsorption of various anionic dyes onto crosslinking PVP hydrogel in dye effluents [22–26]. In these studies, PVP matrix as an adsorbent effectively was used for the removal of anionic dyes.

Carboxylate functions of natural polysaccharides are negatively charged in neutral and alkaline media and hence have greater affinity to cations [27]. It was reported that anionic polysaccharide hydrogels (such as alginate, pectin and carrageenans) were not effective for removal of anionic dyes from wastewaters [17] but in this study, we tried to remove anionic dyes with NaAlg/PVP blend beads. There is no literature studied about NaAlg/PVP hydrogel beads related to dye adsorption. In this study, NaAlg and NaAlg/PVP blend hydrogel beads were prepared by crosslinking method using calcium chloride as a crosslinker. These beads have been used for the removal of dyes such as reactive red 120 (RR), cibacron brilliant red 3B-A (CBR), and remazol brilliant blue R (RBB). The effect of various parameters such as pH, temperature, and initial dye concentration was investigated. The equilibrium adsorption isotherms were described by various isotherm models and also, thermodynamic and kinetic parameters for the adsorption of dyes were investigated.

Experimental

Materials

Reactive Red-120 (chemical formula is $C_{44}H_{24}Cl_2N_{14}O_{20}S_6Na_6$, λ_{max} is 511 nm), CBR (chemical formula is $C_{32}H_{24}ClN_8O_{14}S_4Na_4$, λ_{max} is 517 nm), RBB (chemical formula is $C_{22}H_{16}N_2O_{11}S_3Na_2$, λ_{max} is 590 nm), NaAlg and PVP were obtained from Sigma (Sigma-Aldrich Chemical Co., St. Louis, USA). All other chemicals used in the experiment were of analytical grade.

Preparation of adsorbent beads

2 % (w/w) NaAlg and NaAlg/PVP (containing 80 % NaAlg–20 % PVP w/w) solutions were prepared in distilled water and stirred for 2 h to form homogenous solutions. 50 mL of polymer solutions added drop wise into the 500 mL water containing 2 % (w/v) calcium chloride using a syringe and was allowed to harden in polymer beads with stirring for 30 min. NaAlg and NaAlg/PVP polymer beads were

rinsed three times with distilled water. After, the polymer beads were dried completely at 40 °C under a vacuum to a constant weight.

Batch adsorption experiments

Adsorption experiments were performed using the batch system for the removal of dyes. The effect of various parameters such as pH, initial dye concentration, contact time, and temperature were studied in the orbital shaker at 100 rpm. Stock dye solutions were prepared in distilled water as 1000 mg L⁻¹. The adsorption experiments were carried out by stirring 25 mL dye solution with 0.0325 g of adsorbent beads. The effect of pH onto dye adsorption was studied at various pH ranges between 1.2 and 5.0. The pH of the dye solutions was adjusted with buffer solutions (KCl–HCl for pH = 1.2 and 2.0, potassium biphthalate for pH = 3.0, 4.0, and 5.0). Then, the effect of temperature (25, 35, and 45 °C) and time (60–1080 min) on adsorption of dyes were investigated. Finally, the effect of initial dye concentrations (25–300 mg L⁻¹) on adsorption amount of dyes was studied.

The equilibrium concentrations of dye in the adsorption solutions were estimated spectrophotometrically using UV/Vis spectrophotometer (Shimadzu UV-1800, Japan) by utilizing calibration curves established for each dye.

The adsorption amounts of dyes onto per unit of adsorbent at time (q_t , mg g⁻¹) and equilibrium (q_e , mg g⁻¹) were calculated by using the following Eqs. 1 and 2:

$$q_t = \frac{(C_o - C_t) \times V}{m} \quad (1)$$

$$q_e = \frac{(C_o - C_e) \times V}{m} \quad (2)$$

where C_o , C_e , and C_t represent initial, equilibrium, and t time concentrations of RR, CBR or RBB (mg L⁻¹). V designates the volume of solution (L), and m illustrates mass of adsorbent (g).

Results and discussions

The characterization of the beads

FTIR spectrums of NaAlg beads crosslinked with calcium chloride (A), the NaAlg/PVP blend beads crosslinked with calcium chloride (B), NaAlg/PVP blend beads treated with pH 1.2 buffer solution (C) and pure PVP polymer (D) were shown in Fig. 1. The FTIR spectrum of NaAlg beads (A), the peaks around 3229, 2889, 1590, 1412, 1026 cm⁻¹ were attributed to the stretching of –OH, aliphatic –CH, –COO⁻ (asymmetric), –COO⁻ (symmetric), C–O–C, and the bending of (O–H), respectively. The spectrum of NaAlg/PVP blend beads (B) showed the peaks around 3281, 2923, 1593, 1416, and 1027 cm⁻¹, indicating the stretching of –OH, aliphatic –CH, –COO⁻ (asymmetric), –COO⁻ (symmetric), and C–O–C, respectively. Also, the new

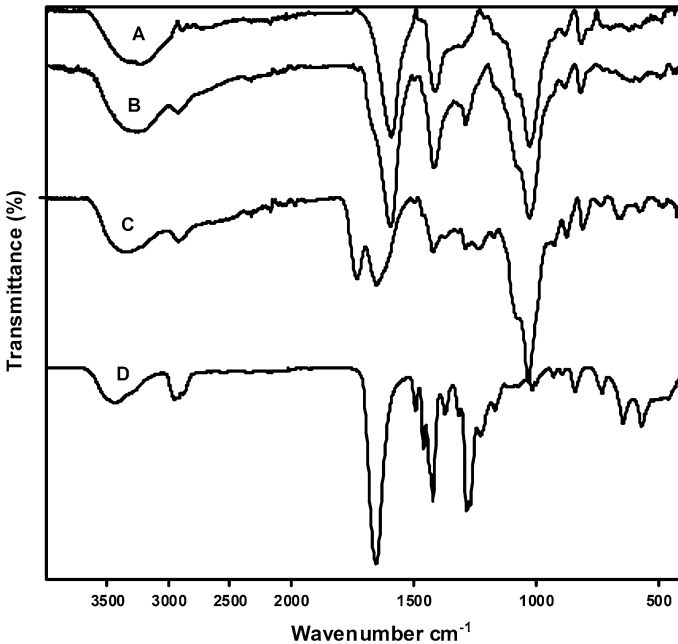


Fig. 1 FTIR spectrums of NaAlg (a), NaAlg/PVP blend (b), NaAlg/PVP blend beads treatment with pH 1.2 buffer solution (c), and pure polymer of PVP (d)

peak around 1286 cm^{-1} was attributed to the bending vibration of (C–N) on the PVP groups [22]. In the spectrum (B), the peak at 1593 cm^{-1} , which belongs to the stretching of $-\text{COO}^-$ (asymmetric), broadened due to overlap the stretching of $-\text{COO}^-$ (asymmetric) on the NaAlg and the stretching of (C=O) on the PVP groups. After the NaAlg/PVP blend beads were treated with pH 1.2 buffer solution (the spectrum C), carboxylic groups of NaAlg were protonated. When the proton displaced by sodium ions, it was observed that the stretching of $-\text{COO}^-$ (asymmetric) on the alginate and (C=O) on the PVP appeared at 1731 and 1652 cm^{-1} , respectively [28]. The observed characteristic peaks of the pure PVP polymer (D) at the FTIR spectrum of the blend beads imply the presence of PVP within the beads after blending with NaAlg.

Thermogravimetric curves of NaAlg beads, NaAlg/PVP blend beads, and pure PVP polymer in a nitrogen atmosphere are shown in Fig. 2. The thermogram of NaAlg beads (A) exhibited important three distinct stages until approximate $600\text{ }^\circ\text{C}$. In the first range, the weight loss from room temperature to $206\text{ }^\circ\text{C}$ was caused by the dehydration of adsorbed water to the hydrophilic polymer beads. In the second and third ranges of $206\text{--}384\text{ }^\circ\text{C}$ and $384\text{--}563\text{ }^\circ\text{C}$ was attributed the decomposition and/or depolymerization of cross linked NaAlg structure and depolymerization of NaAlg [29]. The thermogravimetric curve of NaAlg/PVP hydrogel beads (B) showed three degradation steps until approximate $600\text{ }^\circ\text{C}$. The first in the range from room temperature to $187\text{ }^\circ\text{C}$ was attributed to elimination of adsorbed water of the blend beads. The second in the range of $187\text{--}360\text{ }^\circ\text{C}$ was ascribed to

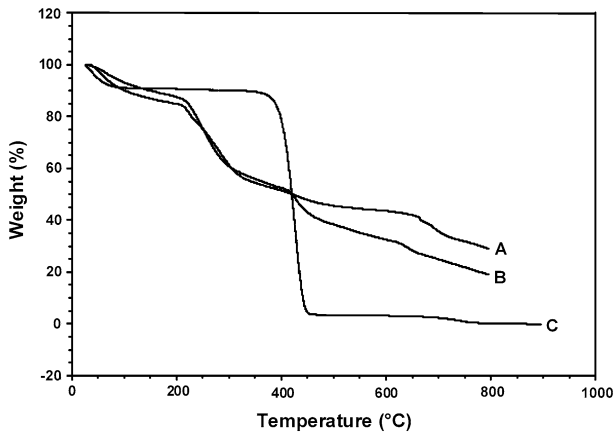


Fig. 2 Thermogravimetric curves of NaAlg beads (a), NaAlg/PVP blend beads (b) and pure polymer of PVP (c)

depolymerization of NaAlg and the decomposition of crosslinking NaAlg structure in blend beads. The third in the range of 360–581 °C was attributed to the decomposition and/or depolymerization of NaAlg and PVP structures. While the weight loss at the thermogram of the NaAlg beads in the range of 384–563 °C is 8.23 %, the weight loss at the thermogram of NaAlg/PVP hydrogel beads in the range of 360–581 °C is 21.63 %. This difference in the thermogravimetric curves of the beads was attributed to the decomposition of PVP polymer chains. Because, the main decomposition curves of pure polymer of PVP (C) was observed between 366 and 461 °C. These results indicated that physical mixtures of polymer chains of PVP and NaAlg in the beads were created [30].

Effect of pH onto dye adsorption

The pH of adsorption solution is one of the most important factors in adsorption studies. The pH of aqueous solution is affected by the chemical structure of dye molecules and functional groups on the surface of adsorbent [31]. The effect of pH on adsorption of dyes was studied for pH values ranging from 1.2 to 5.0 at initial dye concentration of 50 mg L⁻¹, a contact time of 24 h, and at 25 °C. Equilibrium dye uptake capacity (q_e , mg L⁻¹) of the beads has been shown in Fig. 3. As it can be seen from Fig. 3, the adsorption of dyes was not observed in the NaAlg hydrogel beads. Whereas, the highest value of q_e for NaAlg/PVP blend hydrogel beads was obtained at pH 1.2. When the pH of the adsorption solution was increased, the adsorption capacity of blend beads was significantly decreased. Similar results were observed by various adsorption studies on reactive anionic dyes [3, 18, 31–33]. Cheng et al. [33] were studied removal of acid black 1 on amino-polysaccharides and the highest value of q_e was found as pH 3.0. At a low pH, a high electrostatic attraction has been between the positively charged adsorbent and the anionic dye molecules. When the pH of adsorption solution has increased, the number of

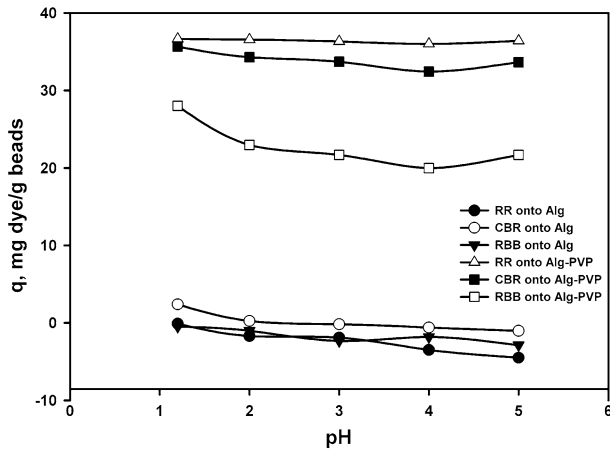


Fig. 3 The effect of pH regimes on the adsorption of NaAlg and NaAlg/PVP beads at initial dye concentration of 50 mg L^{-1}

negatively charged sites increased on the adsorbent molecule and adsorption of dye molecules has decreased due to electrostatic repulsion.

The adsorption of dyes onto the beads clearly changed with the pH of adsorption solution. The functional sodium sulfonate groups onto reactive dye molecules dissociated in aqueous solution as (Dye-SO_3^-) and (Na^+) . As a result of this, dye molecules were loaded with the negative charge. In acidic pH, tertiary amine groups of PVP molecules into the blend beads protonated and loaded with positive charge. As a result of this, the adsorption was occurred through the electrostatic interaction between the two opposite ions (positive charge on nitrogen atom of PVP groups and negative charge on dye anion). However, the adsorption of the dye molecules in high pH solutions was decreased due to the decrease in the electrostatic interaction between the dye anions and the polymeric blend beads cations. When pH was increased, amino groups on the polymeric beads deprotonated and consequently adsorption capacity decreased [3, 25, 32, 33]. A schematic impression of possible electrostatic interaction between negative charge of sulfonate group on the anionic dyes and positive charge of polymer are shown in Fig. 4.

Also, the adsorption capacity has been changed depending on chemical structure of dye molecules. Most affected dye by the change in pH was RBB and the adsorption capacity of beads for RBB decreased 28.68 % with the pH of adsorption solutions increasing from 1.2 to 4. When RBB compared with other dyes, it has least anionic groups. Hence, adsorption capacity of RBB greatly is affected from pH changes and q_e values are lower than the RR and CBR. Similar results were shown in literature [34, 35].

Effect of contact time and temperature onto the dye adsorption

The change of the adsorption of reactive dyes depending on the contact time and temperature were studied in temperature range from 25 to 45 °C, contact time range

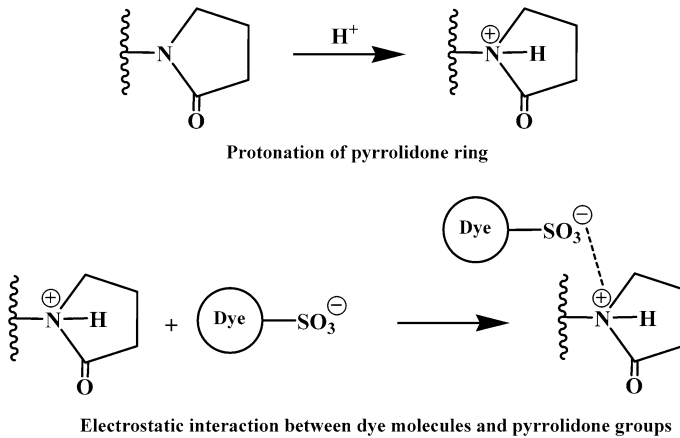


Fig. 4 Schematic impression of possible electrostatic interaction between anionic dyes and polymer beads

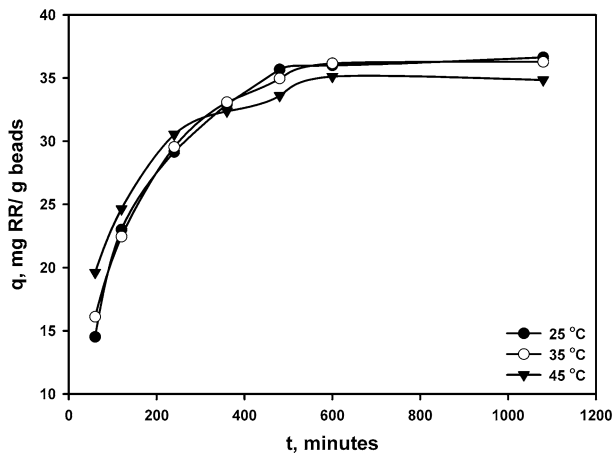


Fig. 5 Effects of contact time and temperature on RR uptake on NaAlG/PVP blend beads at pH 1.2

from 60 to 1080 min, at initial dyes concentration of 50 mg L^{-1} , initial pH of 1.2, and adsorbent beads of 0.0325 g. The effects of contact time and temperature onto the adsorption for polymeric NaAlG/PVP hydrogel beads are illustrated in Figs. 5, 6, and 7.

The contact time between adsorbate and adsorbent is one of the most important variables that affect the adsorption capacity of adsorbent molecules [36]. It can be seen from Figs. 5, 6, and 7 that the adsorption of all dyes was very fast at the first 240 min of the contact time and then it gradually decreased until reaches to an equilibrium stage. The adsorption of all the reactive dyes reached equilibrium stage at 600 min. The fast adsorption in the beginning may be due to existence of a large number of regions available on the surface of the adsorbent for adsorption. After

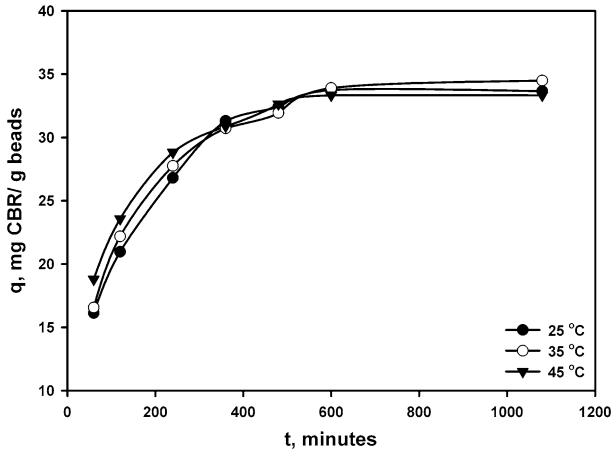


Fig. 6 Effects of contact time and temperature on CBR uptake on NaAlG/PVP blend beads at pH 1.2

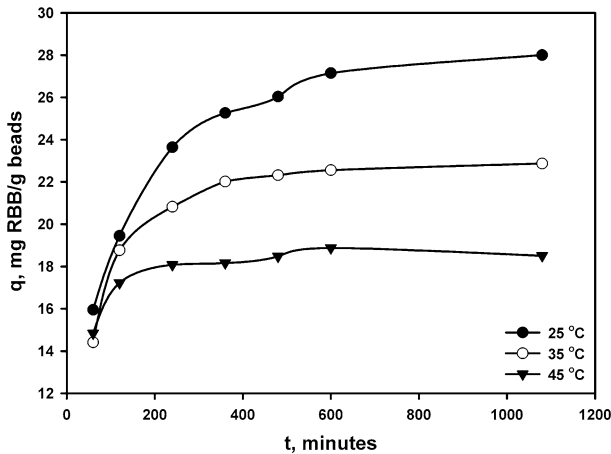


Fig. 7 Effects of contact time and temperature on RBB uptake on NaAlG/PVP blend beads at pH 1.2

240 min of the contact time, adsorption of all the dyes decreased due to the blocking of specific regions for dye adsorption. In other words, after a while, the remaining surface regions were difficult to be occupied because of the repulsion force between the adsorbed dye molecules on the surface of adsorbent and dye molecules in the solution. Also, this may dependent on saturation of active regions as a result of bonding to the outer surface and entrancing into the pores of the hydrogel beads of dye molecules [3, 36, 37]. Çelekli et al. [38] found similar result from adsorption study of Lanaset Red on lentil straw. The adsorption of dye molecules accrued rapidly during first 90 min of contact time and then the adsorption slowed down due to the saturation of binding sites on adsorbent surface [38].

Thermodynamics of the adsorption process can be determined with thermodynamic parameters such as standard free energy (ΔG°), enthalpy (ΔH°), and entropy (ΔS°). The standard free energy (ΔG°) is calculated using the following Eqs. 3 and 4:

$$\Delta G^\circ = \Delta H^\circ - T\Delta S^\circ \quad (3)$$

$$\Delta G^\circ = -RT\ln K_c \quad (4)$$

Van't Hoff equation (Eq. 5) is obtained by combining Eqs. 3 and 4:

$$\ln K_c = \frac{\Delta S^\circ}{R} - \frac{\Delta H^\circ}{RT} \quad (5)$$

where K_c is the equilibrium constant, which is the ratio of the equilibrium concentration of the dye molecules onto adsorbent to the equilibrium concentration of the dye molecules in solution, R is the universal gas constant ($8.314 \text{ J mol}^{-1} \text{ K}^{-1}$) and T is the adsorption temperature (in Kelvin). Values of ΔG° (kJ mol^{-1}) at different temperatures were determined from above equations. The values of ΔH° and ΔS° were calculated from the slope and intercept of the plot between $\ln K_c$ versus $1/T$ ($R^2 > 0.983$) [14].

The Figs. 5, 6, and 7 designate the influence of temperature on capability of adsorption of the NaAlg/PVP blend beads. The calculated thermodynamic parameters are listed in Table 1. It can be seen from Figs. 5, 6, and 7 that the adsorption capacity of RR and CBR dyes did not change with increasing temperature, but the adsorption capacity for the RBB decreased from 28.88 to 18.88 mg g^{-1} with increasing temperature. If the numbers of anionic functional groups on dyes increase, interaction between adsorbent and adsorbate may increase. Anionic groups on RBB are less than RR and CBR. Therefore, electrostatic attraction force between RBB and blend hydrogel beads is lower than the other dyes. Hence, adsorption of RBB molecules onto and/or into adsorbate decreases with increasing temperature. As is known, RR and CBR dyes have a great number of anionic groups. So, the hydrogel beads are strong interaction with the RR and CBR dyes. Their adsorption capacities are higher than RBB and the adsorption capacity has not changed despite increasing temperature. The various adsorption

Table 1 Thermodynamic parameters for the adsorption of all the dyes onto composite hydrogel beads

Dye	T (K)	ΔG° (J mol^{-1})	ΔH° (J mol^{-1})	ΔS° ($\text{J mol}^{-1} \text{ K}^{-1}$)
RR	298	-6322	-24208	-59.8
	308	-5896		
	318	-5118		
CBR	298	-6307	-26644	-68.3
	308	-5539		
	318	-4945		
RBB	298	-2169	-31919	-100.0
	308	-981		
	318	-178		

studies on reactive anionic dyes designated similar results [7, 12, 14]. Regarding the effect of temperature onto adsorption, the obtained results indicated that adsorption of the dyes is physisorption. The calculated thermodynamic parameters (ΔG° , ΔH° , and ΔS°) agreed with these results. The negative values of ΔH° all of dye adsorption demonstrated that the adsorption is exothermic and likely to be physisorption due to the weak electrostatic forces between adsorbent and adsorbate. Besides, recently in reactive dyes adsorption studies, adsorption is described as an exothermic process [12, 14, 39].

The negative values of ΔG° suggested that the adsorption process is spontaneous. In general, the values of standard free energy are in range from -20 to 0 kJ mol^{-1} and from -80 to -400 kJ mol^{-1} for physisorption and chemisorption, respectively [40]. The values of ΔG° in all the adsorption studies changed in range of -6.32 to -0.18 kJ mol^{-1} . In this study, obtained results indicated that the adsorption of all the dyes is spontaneous physisorption [14, 39]. The negative value of ΔS° confirms that the randomness at the solid blend beads/the dye solutions interface decreases during the adsorption of the dyes onto polymeric beads [39].

Vimonses et al. [14] studied thermodynamics of Congo red adsorption onto clay materials and reported that as exothermic and spontaneous physisorption of adsorption process. Asgher and Bhatti [12] were investigated adsorption potential of Citrus waste. They showed that the removal process of anionic dyes (reactive yellow 42, reactive red 45, reactive blue 19 and reactive blue 49) onto these wastes was exothermic and physisorption.

Adsorption kinetics

Various kinetic models have suggested for the elucidation of the adsorption mechanisms of harmful wastes. Pseudo-first-order and pseudo-second-order kinetics models were performed to investigate the dye adsorption mechanisms from aqueous solution onto the NaAlg/PVP beads. The equations related to these models are given as follows Eqs. 6 and 7 [41]:

$$\ln(q_e - q_t) = \ln q_e - k_1 t \text{ (Pseudo-first-order model)} \quad (6)$$

$$\frac{t}{q_t} = \frac{1}{k_2 q_e^2} + \frac{1}{q_e} t \text{ (Pseudo- second-order model)} \quad (7)$$

where, q_e is the equilibrium adsorption capacity (mg g^{-1}), k_1 is the pseudo-first-order rate constant (min^{-1}), q_t is the amount of adsorbed dye (mg g^{-1}) at time t and k_2 is the pseudo-second-order rate constant ($\text{g mg}^{-1} \text{min}^{-1}$). The kinetic parameters for both models at different temperatures are presented in Table 2.

The determined correlation coefficients (R^2 , ranging from 0.992 to 0.999) showed that adsorption processes of dyes onto the beads complied with pseudo-second-order kinetic model. The equilibrium adsorption capacity calculated from the pseudo-second-order model for all of the dyes are compatible with the experimental values [4, 11]. These results have shown that the adsorption of dyes onto the beads at different temperatures is quite compatible for pseudo-second-order kinetic model.

Table 2 Pseudo first and second order rate constant for different temperatures (pH 1.2 and $C_o = 50 \text{ mg L}^{-1}$)

Dye	Temperature ($^{\circ}\text{C}$)	q_{exp}	Pseudo first order kinetic			Pseudo second order kinetic		
			k_1	q_{cal}	R^2	k_2	q_{cal}	R^2
RR	25	36.64	0.00678	33.91	0.982	0.00043	38.83	0.992
	35	36.28	0.00865	45.78	0.928	0.00048	38.31	0.993
	45	35.12	0.00478	17.50	0.967	0.00064	36.11	0.997
CBR	25	35.66	0.00432	24.38	0.991	0.00041	37.31	0.992
	35	34.49	0.00577	26.91	0.957	0.00052	35.97	0.995
	45	33.33	0.00532	18.48	0.982	0.00078	34.36	0.997
RBB	25	28.00	0.00463	14.98	0.987	0.00085	28.82	0.997
	35	22.87	0.00591	9.27	0.977	0.00191	23.31	0.999
	45	18.88	0.00408	3.20	0.873	0.00451	19.01	0.999

Similar results were observed in the variety adsorption studies as the removal of reactive red 120 with *Spirogyra majuscula* [11], remazol brilliant blue R with peanut hull-based activated carbon [41], remazol brilliant orange 3R with coffee husk-based activated carbon [37], three anionic dyes (methyl orange, brilliant yellow, and alizarin red) with magnetic-sulfonic graphene nanocomposite [42].

Effect of initial concentration onto the dye adsorption

Initial concentration in adsorption studies which is one of the most important parameters affecting mass transfer between aqueous solution and solid adsorbent. However, mass transfer affects the uptake capacity of adsorbent molecules [3, 11, 43]. The anionic dyes uptake capacity of the polymeric blend beads was investigated at various initial dye concentrations ($C_o = 25\text{--}300 \text{ mg L}^{-1}$). The effect of initial dye concentrations on the adsorption of all the dyes is shown in Fig. 8. According to the results presented in Fig. 8, the equilibrium adsorption capacity increased with increasing initial dye concentration from 25 to 200 mg L^{-1} (for the CBR and the RBB dyes) and from 25 to 250 mg L^{-1} (for the RR dye). Similar results were found in the literature [3, 7, 37]. This result can be attributed to an increase in the initial dye concentration that is accelerated the mass transfer between dye solution and adsorbent, and thus behaves as a driving force for the transfer of dye molecules from dye solution to the surface of the beads [14, 37]. Also, the dye uptake capacity of the blend beads increases depending on the increase of the dye concentration due to more interactions or more collision between the adsorbate dye molecules with the adsorbent beads [7, 39]. But, after a certain concentration of the dyes, dye uptake capacity of the beads reaches a constant value because there are no active regions for the adsorption on the surface of the beads or adsorption regions coated with the dyes molecules. This trend is compatible with earlier studies related to anionic dyes adsorption such as reactive black 5 onto chitosan [44], Lanaset Red on lentil straw [38].

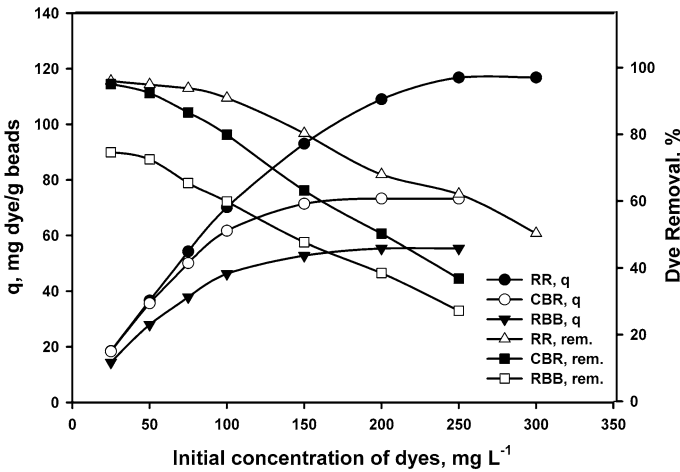


Fig. 8 Effects of initial dye concentration on RR, CBR, and RBB uptake on NaAlg/PVP blend beads at pH 1.2

Adsorption isotherm

The most important data obtained from the equilibrium adsorption isotherms to explain the mechanism of adsorption process. The most widely isotherm models which Langmuir and Freundlich isotherms were employed to explain adsorption process. A Langmuir isotherm base on the adsorption of molecules occurs as monolayer on a homogeneous surface [3].

The linearized equation for the Langmuir isotherm is given by the following Eq. 8:

$$\frac{C_e}{q_e} = \frac{1}{q_{max}K_L} + \frac{C_e}{q_{max}} \tag{8}$$

where C_e is the equilibrium dye concentration in adsorption solution (mg L^{-1}), q_{max} is the adsorption capacity (mg g^{-1}) and K_L is the Langmuir constant (L mg^{-1}). The essential characteristics of Langmuir dimensionless constant separation factor, R_L are defined by the following Eq. 9 [45]:

$$R_L = \frac{1}{1 + K_L C_o} \tag{9}$$

where C_o is the initial concentration of adsorption solution (mg L^{-1}). The adsorption process depending on the value of R_L is unfavorable ($R_L > 1.0$), linear ($R_L = 1.0$), favorable, ($1 > R_L > 0$) or irreversible ($R_L = 0$) [18].

Freundlich isotherm is a model that describes as multilayer of adsorption of molecules on the heterogeneous adsorbent surface and is calculated with follows Eq. 10:

Table 3 Langmuir and Freundlich isotherm parameters, correlation coefficients and values of separation factor (R_L) for the adsorption of all the dyes onto composite hydrogel beads

Dye	q_{exp}	q_{max}	Langmuir isotherm			Freundlich isotherm		
			K_L (L mg ⁻¹)	R^2	R_L	K_F	n	R^2
RR	117.90	121.51	0.192	0.998	0.0945	26.58	2.95	0.911
CBR	74.31	75.82	0.294	0.999	0.1138	31.11	5.24	0.902
RBB	56.42	60.24	0.082	0.992	0.1959	15.61	3.78	0.900

$$q_e = K_F C_e^{1/n} \quad (10)$$

where K_F is the Freundlich constant and n is heterogeneity factor.

Adsorption isotherm constants, values of correlation coefficients and separation factor values (R_L) presented in Table 3. The results obtained from experimental data showed that the adsorption of dyes meets to Langmuir isotherm model compared with the Freundlich isotherm model. The results of adsorption isotherm all of the dyes for the blend beads provided a very good fit to Langmuir isotherm model because of the high correlation coefficients ($R^2 = 0.992$ – 0.998). The Langmuir isotherm indicated that each of active sites on the surface of the adsorbent is capable of adsorbing alone single one dye molecule. In addition, the q_{max} values calculated from Langmuir isotherm were suitable with experimental q_{exp} values. The values of R_L (0.0945–0.1959) observed in the range of 0–1 and confirmed the adsorption process for blend beads is favorable [11, 46]. The similar results reported in the variety literatures such as the adsorption of Acid Red 111 on natural and activated vine stem [47], Congo Red from aqueous solutions on Perlite [48], Reactive Black 5 from aqueous solution onto chitosan [44] and Congo Red onto chitosan/poly(vinyl alcohol) hydrogel beads [18].

Column studies with real dye effluent

Column tests were carried out for determine the adsorption capacity of NaAlg/PVP blend beads for removing of reactive dyes from textile effluent under continuous flow conditions of dye solution. A glass column (length and diameter 50 cm × 1.3 cm) was filled with NaAlg/PVP blend beads. Textile wastewater containing the RR (obtained from a textile company, Kestel, Bursa, Turkey) was used during this experiment. Dye concentration and pH value in the textile effluent solution was measured as 137.20 ppm and 10.1, respectively. Then, pH value of this solution was adjusted as 5.0 using 1 M HCl solution and dye concentration of wastewater almost unchanged. Flow rate of dye solution from column was adjusted as 5 mL/min using a peristaltic pump (Cole-parmer, Masterflex L/S, USA). The equilibrium adsorption capacity and removal percentage were found 44.26 mg g⁻¹ and 75.01 %, respectively. The equilibrium adsorption capacity and removal percentage values in the initial dye concentration study (Part: Effect of initial dye concentration onto the adsorption) of 150 ppm synthetic RR solution in batch

Table 4 Comparison of maximum adsorption capacities of various adsorbents for removal of RR, CBR, and RBB

Adsorbent	Studied parameters	Dye	q_{\max} (mg g ⁻¹)	References
Seashell wastes	$C_o = 300$ mg L ⁻¹ $V = 25$ mL $m = 6$ g L ⁻¹	RR	27.70	[50]
<i>Lentinus sajor-caju</i>	$C_o = 800$ mg L ⁻¹ $V = 50$ mL $m = 1$ mg mL ⁻¹	RR	182.90	[4]
Furnace slag	$C_o = 500$ mg L ⁻¹ $V = 100$ mL $m = 5$ mg mL ⁻¹	RR	55.00	[31]
NaAlg/PVP beads	$C_o = 300$ mg L ⁻¹ $V = 25$ mL $m = 0.0325$ g	RR	116.82	Present work
Immobilized chitosan on glass plates	$C_o = 80$ mg L ⁻¹ $V = 30$ mL $m = 20$ mg	CBR	104.88	[51]
Coke waste	$C_o = 900$ mg L ⁻¹ $V = 30$ mL $m = 0.15$ g	CBR	70.30	[52]
Protonated sludge	$C_o = 900$ mg L ⁻¹ $V = 30$ mL $m = 0.15$ g	CBR	73.70	[53]
NaAlg/PVP beads	$C_o = 250$ mg L ⁻¹ $V = 25$ mL $m = 0.0325$ g	CBR	73.26	Present work
Peanut hull-based activated carbon	$C_o = 300$ mg L ⁻¹ $V = 25$ mL $m = 0.04$ g	RBB	149.25	[41]
Fly ash	$C_o = 500$ mg L ⁻¹ $V = 50$ mL $m = 0.3$ g	RBB	165.00	[54]
Activated sepiolite	$C_o = 200$ mg L ⁻¹ $V = 25$ mL $m = 0.5$ g	RBB	9.94	[55]
NaAlg/PVP beads	$C_o = 250$ mg L ⁻¹ $V = 25$ mL $m = 0.0325$ g	RBB	55.28	Present work

C_o initial dye concentration, V volume of adsorption solution, m mass of adsorbent

system were determined as 93.00 mg g⁻¹ and 80.60 %, respectively. When the q_e values of the 150 ppm RR solution in batch system compared with column system, q_e values of column about half of batch system. This result can be attributed to the

effect of salt. Salts which were added in textile dye solutions may be reduced the adsorption of RR. Consequently, the anions in salt adsorbed on positively charged active PVP groups and the adsorption of RR molecules on blend beads decreased [49].

Comparison of various adsorbents

Comparisons of maximum adsorption capacities of various adsorbents for removal of dyes were summarized in Table 4. The q_{\max} values observed that NaAlg/PVP hydrogel beads may be useful adsorbent the removal of reactive anionic dyes. The materials used for preparation of hydrogel beads have biocompatible, biodegradable, non-toxic properties and the advantages of these materials were given in various adsorption studies [4, 17, 18, 27, 31, 33, 41, 44, 50–55].

Conclusions

The anionic alginate hydrogels were not used effectively in removal of anionic dyes from wastewaters. Therefore, in this study, blend hydrogel beads of NaAlg/PVP were prepared and these beads have been used for removal of RR, CBR, and RBB. The maximum adsorption capacities were found 116.82 mg g⁻¹ for RR, 73.26 mg g⁻¹ for CBR, and 55.28 mg g⁻¹ for RBB. The adsorption is exothermic and likely to be physisorption. The obtained NaAlg/PVP blend beads may be used effectively in the removal of anionic dyes from textile wastewaters.

Acknowledgments The authors gratefully acknowledge the financial support provided by the Kırıkkale University Research Fund through Project 2011/2.

References

1. Vijayaraghavan K, Yun YS (2008) Biosorption of C.I. reactive black 5 from aqueous solution using acid treated biomass of brown seaweed *Laminaria* sp. *Dyes Pigments* 76:726–732
2. Aksu Z (2005) Application of biosorption for the removal of organic pollutants: a review. *Process Biochem* 40:997–1026
3. Çelekli A, İlgin G, Bozkurt H (2012) Sorption equilibrium, kinetic, thermodynamic, and desorption studies of reactive red 120 on *Characontraria*. *Chem Eng J* 191:228–235
4. Arica MY, Bayramoğlu G (2007) Biosorption of reactive red-120 dye from aqueous solution by native and modified fungus biomass preparations of *Lentinussajor-caju*. *J Hazard Mater* 149:499–507
5. Acar I, Bal A, Güçlü G (2012) Adsorption of basic dyes from aqueous solutions by depolymerization products of post-consumer PET bottles. *Clean Soil Air Water* 40:325–333
6. Khaled A, El Nemr A, El-Sikaily A, Abdelwahap O (2009) Removal of direct N-Blue-106 from artificial textile dye effluent using activated carbon from orange peel: adsorption isotherm and kinetic studies. *J Hazard Mater* 165:100–110
7. Jesus AMD, Romão LPC, Araújo BR, Costa AS, Marques JJ (2011) Use of humin as an alternative material for adsorption/desorption of reactive dyes. *Desalination* 274:13–21
8. Sadettin S, Donmez G (2006) Bioaccumulation of reactive dyes by thermophilic cyanobacteria. *Process Biochem* 41:836–841
9. Aksu Z, Tezer S (2005) Biosorption of reactive dyes on the green alga *Chlorella vulgaris*. *Process Biochem* 40:1347–1361

10. Bhatti HN, Arkam N, Asgher M (2008) Optimization of culture conditions for enhanced decolorization of cibacron red FN-2BL by *Schizophyllum commune* IBL-6. *Appl Biochem Biotechnol* 149:255–264
11. Çelekli A, Yavuzatmaca M, Bozkurt H (2009) Kinetic and equilibrium studies on the adsorption of reactive red 120 from aqueous solution on *Spirogyra majuscula*. *Chem Eng J* 152:139–145
12. Asgher M, Bhatti HN (2012) Evaluation of thermodynamics and effect of chemical treatments on sorption potential of Citrus waste biomass for removal of anionic dyes from aqueous solutions. *Ecol Eng* 38:79–85
13. Chowdhury AK, Sarkar AD, Bandyopadhyay A (2009) Rice husk ash as a low cost adsorbent for the removal of methylene blue and congo red in aqueous phases. *Clean Soil Air Water* 37:581–591
14. Vimonses V, Lei S, Jin B, Chris WKC, Chris S (2009) Kinetic study and equilibrium isotherm analysis of Congo red adsorption by clay materials. *Chem Eng J* 148:354–364
15. Babu VR, Sairam M, Hosamani KM, Aminabhavi TM (2007) Preparation of sodium alginate–methylcellulose blend microspheres for controlled release of nifedipine. *Carbohydr Polym* 69:241–250
16. Akamatsu K, Maruyama K, Chen W, Nakao A, Nakao S (2011) Drastic difference in porous structure of calcium alginate microspheres prepared with fresh or hydrolyzed sodium alginate. *J Colloid Interface Sci* 363:707–710
17. Blackburn R (2004) Natural polysaccharides and their interactions with dye molecules: applications in effluent treatment. *Environ Sci Technol* 38:4905–4909
18. Zhu HY, Fu YQ, Jiang R, Yao J, Xiao L, Zeng GM (2012) Novel magnetic chitosan/poly(vinyl alcohol) hydrogel beads: preparation, characterization and application for adsorption of dye from aqueous solution. *Bioresour Technol* 105:24–30
19. Yan L, Chang PR, Zheng P, Yan XML, Chang PR, Zheng P, Ma X (2012) Characterization of magnetic guar gum-grafted carbon nanotubes and the adsorption of the dyes. *Carbohydr Polym* 87:1919–1924
20. Fan J, Shi Z, Lian M, Li H, Yin J (2013) Mechanically strong graphene oxide/sodium alginate/polyacrylamide nanocomposite hydrogel with improved dye adsorption capacity. *J Mater Chem A* 1:7433–7443
21. Bhattacharyya R, Ray SK (2014) Adsorption of industrial dyes by semi-IPN hydrogels of acrylic copolymers and sodium alginate. *J Ind Eng Chem*. doi:10.1016/j.jiec.2014.06.029
22. Wang W, Wang A (2010) Synthesis and swelling properties of pH-sensitive semi-IPN superabsorbent hydrogels based on sodium alginate-g-poly(sodium acrylate) and polyvinylpyrrolidone. *Carbohydr Polym* 80:1028–1036
23. Lu Q, Yu J, Gao J, Yang W, Li Y (2011) Glow-discharge electrolysis plasma induced synthesis of polyvinylpyrrolidone/acrylic acid hydrogel and its adsorption properties for heavy-metal ions. *Plasma Process Polym* 8:803–814
24. Wang W, Wang Q, Wang A (2011) pH-responsive carboxymethylcellulose-g-poly(sodium acrylate)/polyvinylpyrrolidone semi-IPN hydrogels with enhanced responsive and swelling properties. *Macromol Res* 19:57–65
25. Saraydın D, Karadağ E (2000) Binding of some dyes onto crosslinked poly (*N*-vinylpyrrolidone). *Polym Bull* 44:501–508
26. Şenkal BF, Erkal D, Yavuz E (2006) Removal of dyes from water by poly(vinyl pyrrolidone) hydrogel. *Polym Adv Technol* 17:924–927
27. Rocher V, Siaugue JM, Cabuil V, Bee A (2008) Removal of organic dyes by magnetic alginate beads. *Water Res* 42:1290–1298
28. Pathak TS, Kim JS, Lee SJ, Baek DJ, Paeng J (2008) Preparation of alginic acid and metal alginate from algae and their comparative study. *J Polym Environ* 16:198–204
29. Işıklı N, Kurşun F, İnal M (2010) Graft copolymerization of itaconic acid onto sodium alginate using benzoyl peroxide. *Carbohydr Polym* 79:665–672
30. Moharram MA, Khafagi MG (2006) Thermal behavior of poly(acrylic acid)–poly(vinyl pyrrolidone) and poly(acrylic acid)–metal–poly(vinyl pyrrolidone) complexes. *J Appl Polym Sci* 102:4049–4057
31. Xue Y, Hou H, Zhu S (2009) Adsorption removal of reactive dyes from aqueous solution by modified basic oxygen furnace slag: isotherm and kinetic study. *Chem Eng J* 147:272–279
32. Çelekli A, Tanrıverdi B, Bozkurt H (2011) Predictive modeling of removal of Lanaset Red G on *Chara contraria*; kinetic, equilibrium, and thermodynamic studies. *Chem Eng J* 169:166–172
33. Cheng R, Jiang Z, Ou S, Li Y, Xiang B (2009) Investigation of acid black 1 adsorption onto amino-polysaccharides. *Polym Bull* 62:69–77

34. Min M, Shen L, Hong G, Zhu M, Zhang Y, Wang X, Chen Y, Hsiao BS (2012) Micro-nano structure poly(ether sulfones)/poly(ethyleneimine) nanofibrous affinity membranes for adsorption of anionic dyes and heavy metal ions in aqueous solution. *Chem Eng J* 197:88–100
35. Zhao S, Zhou F, Li L, Cao M, Zuo D, Liu H (2012) Removal of anionic dyes from aqueous solutions by adsorption of chitosan-based semi-IPN hydrogel composites. *Composites B* 43:1570–1578
36. Absalan G, Asadi M, Kamran S, Sheikhan L, Goltz DM (2011) Removal of reactive red-120 and 4-(2-pyridylazo) resorcinol from aqueous samples by Fe₃O₄ magnetic nanoparticles using ionic liquid as modifier. *J Hazard Mater* 192:476–484
37. Ahmad MA, Rahman NK (2011) Equilibrium, kinetics and thermodynamic of remazol brilliant orange 3R dye adsorption on coffee husk-based activated carbon. *Chem Eng J* 170:154–161
38. Çelekli A, Tanrıverdi B, Bozkurt H (2012) Lentil straw: a novel adsorbent for removing of hazardous dye-sorption behavior studies. *Clean Soil Air Water* 40:515–522
39. Aravindhan R, Rao JR, Nair BU (2007) Removal of basic yellow dye from aqueous solution by sorption on green alga *Caulerpa scalpelliformis*. *J Hazard Mater* 142:68–76
40. Chu BS, Baharin BS, Man YBC, Quek SY (2004) Separation of vitamin E from palm fatty acid distillate using silica: I equilibrium of batch adsorption. *J Food Eng* 62:97–103
41. Zhong ZY, Yang Q, Li XM, Luo K, Liu Y, Zeng GM (2012) Preparation of peanut hull-based activated carbon by microwave-induced phosphoric acid activation and its application in remazol brilliant blue R adsorption. *Ind Crop Prod* 37:178–185
42. Wang S, Wei J, Lv S, Guo Z, Jiang F (2013) Removal of organic dyes in environmental water onto magnetic-sulfonic graphene nanocomposite. *Clean Soil Air Water* 41:992–1001
43. Naveen N, Saravanan P, Baskar G, Renganathan S (2011) Equilibrium and kinetic modeling on the removal of reactive red 120 using positively charged *Hydrilla verticillata*. *J Taiwan Inst Chem E* 42:463–469
44. Saha TK, Bhoumik NC, Karmaker S, Ahmed MG, Ichikawa H, Fukumori Y (2011) Adsorption characteristics of reactive black 5 from aqueous solution onto chitosan. *Clean Soil Air Water* 39:984–993
45. Sathishkumara P, Arulkumar B, Palvannan T (2012) Utilization of agro-industrial waste *Jatropha curcas* pods as an activated carbon for the adsorption of reactive dye remazol brilliant blue R (RBBR). *J Clean Prod* 22:67–75
46. Luo X, Zhang L (2009) High effective adsorption of organic dyes on magnetic cellulose beads entrapping activated carbon. *J Hazard Mater* 171:340–347
47. Ayan EM, Toptaş A, Kıbrıslıoğlu G, Yalçınkaya EES, Yanık J (2011) Biosorption of dyes by natural and activated vine stem. Interaction between biosorbent and dye. *Clean Soil Air Water* 39:406–412
48. Vijayakumar G, Dharmendrakumar M, Renganathan S, Sivanesan S, Baskar G, Elango KP (2009) Removal of Congo Red from aqueous solutions by Perlite. *Clean Soil Air Water* 37:355–364
49. Eren E (2010) Adsorption performance and mechanism in binding of azo dye by raw bentonite. *Clean Soil Air Water* 38:758–763
50. Suteu D, Bilba D, Aflori M, Doroftei F, Lisa G, Badeanu M, Malutan T (2012) The seashell wastes as biosorbent for reactive dye removal from textile effluents. *Clean Soil Air Water* 40:198–205
51. Nawi MA, Sabar S, Sheilatina AHJ, Ngah WSW (2010) Adsorption of Reactive Red 4 by immobilized chitosan on glass plates: towards the design of immobilized TiO₂-chitosan synergistic photocatalyst-adsorption bilayer system. *Biochem Eng J* 49:317–325
52. Won SW, Wu G, Ma H, Liu Q, Yan Y, Cui L, Liu C, Yun YS (2006) Adsorption performance and mechanism in binding of reactive red 4 by coke waste. *J Hazard Mater* 138:370–377
53. Junxiong C, Longzhe C, Yanxin W, Chengfu L (2009) Effect of functional groups on sludge for biosorption of reactive dyes. *J Environ Sci* 21:534–538
54. Dizge N, Aydinler C, Demirbaş E, Konya M, Kara S (2008) Adsorption of reactive dyes from aqueous solutions by fly ash: kinetic and equilibrium studies. *J Hazard Mater* 150:737–746
55. Uğurlu M (2009) Adsorption of a textile dyes onto activated sepiolite. *Microporous Mesoporous Mater* 119:276–283